Coherent Optical 25.8-Gb/s OFDM Transmission Over 4160-km SSMF

Sander L. Jansen, *Member, IEEE*, Itsuro Morita, Tim C. W. Schenk, *Member, IEEE*, Noriyuki Takeda, and Hideaki Tanaka

***Abstract*—We discuss coherent optical orthogonal frequency division multiplexing (CO-OFDM) as a suitable modulation technique for long-haul transmission systems. Several design and implementation aspects of a CO-OFDM system are reviewed, but we especially focus on phase noise compensation. As conventional CO-OFDM transmission systems are very sensitive to laser phase noise a novel method to compensate for phase noise is introduced. With the help of this phase noise compensation method we show continuously detectable OFDM transmission at 25.8 Gb/s data rate (20 Gb/s after coding) over 4160-km SSMF without dispersion compensation.**

***Index Terms*—Chromatic dispersion compensation, fiber-optic transmission systems, long-haul transmission, orthogonal frequency division multiplexing (OFDM).**

I. Introduction

ORTHOGONAL FREQUENCY DIVISION MULTIPLEXING (OFDM) is a promising method to eliminate the need for optical dispersion compensation in long-haul transmission links. Fiber-optic OFDM systems can be realized either with direct detection optical (DDO) [1], [2] or with coherent optical (CO) detection [3], [4]. Recently, several high data rate OFDM transmission experiments have been reported. With DDO-OFDM, 20 Gb/s transmission over 320 km standard single mode fiber (SSMF) was shown by Brendon *et al.* [1] and a directly modulated laser was used by Lee *et al.* to transmit 24.1 Gb/s over 730 m of multimode fiber [2]. Using CO-OFDM, Shieh *et al.* [3] demonstrated 8-Gb/s over 1000 km of SSMF and recently, we reported long-haul 25.8-Gb/s transmission over 4160 km of SSMF [4].

Whereas DDO-OFDM is more suitable for cost-effective short reach applications, the superior performance of CO-OFDM makes it an excellent candidate for long-haul transmission systems. The sensitivity of CO-OFDM is superior to that of DDO-OFDM as DDO-OFDM requires half the optical power to be allocated for the transmission of the carrier. DDO-OFDM furthermore requires that a guard band is used between the optical carrier and the OFDM band, in order to avoid intermodulation impairments that occur at the photodiode [1]. This guard band effectively halves the obtainable (optical) spectral efficiency and increases the bandwidth requirements of the optical front end of the transmitter and receiver. On the other hand, DDO-OFDM requires fewer components at transmitter and receiver than CO-OFDM and is therefore more cost-effective. A major concern of CO-OFDM is the phase noise of the local oscillator that must be compensated for, especially since the impact of phase noise on the performance of OFDM systems is much larger than that of thermal noise [5].

In conventional CO-OFDM systems, phase noise is partly suppressed by estimating the local oscillator (LO) offset using the cyclic prefix or training symbols. In such transmission systems the influence of phase noise must be reduced by using a small fast Fourier transform (FFT) size and lasers with narrow linewidths (for instance 128 FFT size and 40-kHz linewidth in [3]). However, narrow linewidth lasers are in general expensive and a larger FFT size is preferable in an OFDM system as it reduces the relative overhead of the cyclic prefix.

Recently, we proposed a new method to compensate for laser phase noise in which a low-power RF-pilot tone is used to revert the phase noise impairments at the receiver. With this scheme, transmission of 25.8 Gb/s over 4160 km has been realized [4]. Furthermore, it has been shown that 12.5-Gb/s OFDM can be realized with large FFT size (1024 FFT) using conventional DFB lasers (5 MHz linewidth) [6]. Compared to the configuration with ECL lasers (100 kHz linewidth) an OSNR penalty of only 1 dB is observed in this experiment.

In this paper, we elaborate on [4] and discuss in more detail the transmission experiment of 25.8 Gb/s (20 Gb/s after coding) CO-OFDM over 4160 km. The paper is structured as follows. In Section II the most important design aspects of a CO-OFDM transmission system are discussed. Subsequently, a detailed description of the phase noise compensation scheme is described in Section III. The experimental setup for the long-haul OFDM transmission experiment is given in Section IV and the experimental results are discussed in Section V. A brief outlook is presented in Section VI and in Section VII we draw the conclusions.

II. OFDM System Design

The basic concept behind OFDM is the division of a high bitrate data stream into several low bitrate streams by using block transmission. Fig. 1 shows the block diagram of a typical OFDM transmitter and receiver. A binary data stream is converted from serial to parallel and after symbol mapping the low bitrate streams are simultaneously modulated onto orthogonal carriers. The orthogonality between the carriers is realized by spacing the carriers with a multiple of the symbol duration (of the low bitrate streams). A very effective way of generating the OFDM subcarriers is by taking the IFFT. After the IFFT, cyclic

Manuscript received June 29, 2007; revised September 6, 2007. This work was supported in part by a project of the National Institute of Information and Communications Technology of Japan.

S. L. Jansen, I. Morita, N. Takeda, and H. Tanaka are with the KDDI R&D Laboratories, Saitama 3568502, Japan (e-mail: SL-Jansen@kddilabs.jp).

T. C. W. Schenk is with Philips Research, Eindhoven, 5656 AE, The Netherlands (e-mail: tim.schenk@philips.com).

Digital Object Identifier 10.1109/JLT.2007.911888

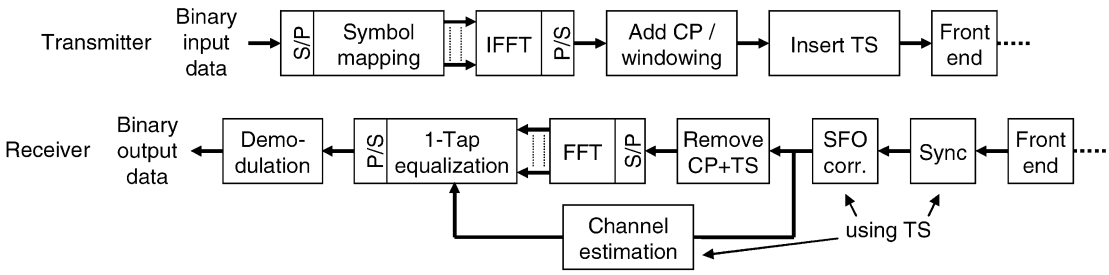

Fig. 1. Block diagram of a typical OFDM transmitter and receiver, with CP = cyclic prefix, TS = training symbol, Sync. = Symbol Synchronization, SFO = sample frequency offset, P = parallel and S = serial.

prefix and training symbols are added and the signal is fed to the front end. In the case of fiber-optic OFDM, this is an optical modulator.

At the receiver, the front end consists of either coherent or direct detection. Subsequently, training symbols are used for symbol synchronization and for the compensation of several impairments (discussed in Section II-B). The OFDM signal is then converted back to the frequency domain by taking the FFT. Finally, the binary data is recovered by demodulating (or demapping) the equalized signal. This demodulation block is the slicer of the receiver and can either be implemented with soft or hard decision coding [7].

Numerous system parameters are critical for the design of an OFDM system. In this section, some of the most important parameters and tradeoffs are discussed. Note that phase noise compensation is required when optical coherent detection is used at the receiver. In this section, general design aspects are discussed which are valid for both CO-OFDM and DDO-OFDM. Phase noise compensation for CO-OFDM systems is discussed in detail in Section III and for simplicity omitted from the block diagram shown in Fig. 1.

A. FFT Size

Probably the most important parameter of an OFDM system is the FFT size as it determines the number of subcarriers of the OFDM system. In complex-valued OFDM systems [3], [4] the FFT size equals the number of subcarriers, whereas in real-valued OFDM systems [1], [2] the number of generated subcarriers equals half the FFT-size because of the required Hermitian symmetry. The FFT size is normally a power of two and common values for the FFT size are between 128 [3] and 1024 [2]. Increasing the FFT size reduces the symbol rate and makes the signal as such less vulnerable to inter-symbol interference (ISI) along the transmission link. A second advantage of a large FFT size is that it reduces the relative overhead of the cyclic prefix (further discussed in Section II.C). On the other hand, the main drawback of a large FFT size is that it increases the processing complexity at the transmitter and receiver [8]. Furthermore, for systems employing coherent detection at the receiver, a higher FFT-size results in an increased sensitivity to laser phase noise [9].

B. Training Symbols

Training symbols are required in an OFDM signal in order to find the symbol boundaries, e.g., for symbol synchronization. A common training-symbol implementation is by using two OFDM symbols with the same, known data sequence. As the two training symbols have the same data, they are highly correlated and, thus, synchronization can be realized by correlating between subsequent symbols [10], [11]. The training block is furthermore used to derive the coefficients for the 1-tap equalizer, which compensates for timing offset and the distortions of the transmission path (for example, chromatic dispersion). These coefficients are found by comparing the received training symbol with the original one. This technique is commonly referred to as channel estimation and described in detail in [10] and [11]. By using training symbols also, the sampling frequency offset (SFO) between the transmitter and the receiver can be compensated for. This technique is discussed in detail in [12].

In general, a large training block spacing (i.e., the number of symbols between each training symbol) is preferable as this reduces the overhead. However, a large training block spacing reduces the speed with which the OFDM system can adapt to fast changes in the fiber-optic network, caused for example by polarization dependent loss (PDL). When N_{Training} represents the number of OFDM training symbols used per training block and N_{Tr_spacing} the training block spacing, the training overhead $\varepsilon_{\mathrm{Training}}$ can be expressed as

$$\varepsilon_{\mathrm{Training}} = \frac{N_{\mathrm{Training}}}{N_{Tr\_\mathrm{spacing}}}. \tag{1}$$

C. Cyclic Prefix

Applying a cyclic prefix (sometimes referred to as cyclic extension or guard interval) is an effective technique to eliminate virtually all ISI in an OFDM transmission system. The source of the ISI could for example be chromatic dispersion or polarization mode dispersion (PMD) along the transmission link. Furthermore, a cyclic prefix is needed to compensate for offsets in the symbol synchronization. A cyclic prefix is realized by copying the last N_g samples of each OFDM symbol and adding them to the beginning of that same symbol. The constant N_g is commonly referred to as the guard interval length or guard time (in samples).

As the cyclic prefix itself contains redundant information, it introduces overhead into the OFDM system. In order to minimize this overhead, a short guard time is preferable. The main tradeoff when choosing the guard time is, therefore, between ISI robustness and net data rate. It has been shown that the minimum

guard time T_g required to eliminate all ISI caused by chromatic dispersion and differential group delay (DGD) can be expressed as [13]

$$\frac{c}{f_c^2} \cdot |D| \cdot N_c \cdot \Delta f + \mathrm{DGD}_{\mathrm{MAX}} \leqslant T_g \tag{2}$$

where f_c is the optical carrier frequency, c is the speed of light, D is the total amount of chromatic dispersion, $\mathrm{DGD}_{\mathrm{MAX}}$ is the maximum budgeted DGD, N_c is the number of subcarriers, and Δf is the subcarrier channel spacing. Note that the maximum DGD can be approximated by about 3.5 times the mean PMD in typical fiber installations and that N_c equals the OFDM symbol length in samples (excluding cyclic prefix). The minimum guard interval required, expressed in samples N_g, can then be written as

$$T_g \cdot N_c \cdot \Delta f = T_g \cdot f_s = N_g \tag{3}$$

where f_s is the sample frequency of the DAC used to generate the signal. The overhead induced by cyclic prefix $\varepsilon_{\mathrm{Cyclic}}$ can then be expressed as

$$\varepsilon_{\mathrm{Cyclic}} = \frac{N_g}{N_c}. \tag{4}$$

D. Data Rate

Both training symbols and cyclic prefix introduce overhead to the OFDM system. Therefore, in any OFDM system, the useful data rate for data transmission (net data rate) is lower than the data rate before coding. The data rate before coding is commonly referred to as the nominal data rate R_{Nominal}. Taking the overhead for cyclic prefix and training symbols into account, the raw data rate can be expressed as

$$R_{\mathrm{Raw}} = R_{\mathrm{Nominal}} \cdot \frac{1}{(1+\varepsilon_{\mathrm{Training}})} \cdot \frac{1}{(1+\varepsilon_{\mathrm{Cyclic}}).} \tag{5}$$

In the raw data, the forward error correction (FEC) overhead is not considered. The data rate after FEC is the net data rate R_{Net}. This data rate is referred to as well as the data rate after coding and can be written as

$$R_{\mathrm{Net}} = R_{\mathrm{Raw}} \cdot \frac{1}{(1+\varepsilon_{\mathrm{FEC}})} \tag{6}$$

where $\varepsilon_{\mathrm{FEC}}$ represents the overhead induced by FEC coding. As the overhead for FEC code, cyclic prefix and training symbols is dependent on the system configuration, the exact overhead is different for each OFDM system.

In the transmission experiment described in this paper, the data rate before coding is $R_{\mathrm{Nominal}} = 25.8$ Gb/s. The FFT size is $N_c = 256$ and the cyclic prefix is $N_g = 27$ samples per symbol resulting in an overhead of $\varepsilon_{\mathrm{Cyclic}} \cong 10.5\%$. Two training symbols ($N_{\mathrm{Training}} = 2$) are inserted every 25 data symbols ($N_{Tr\_\mathrm{spacing}} = 25$) and thus the overhead caused by training symbols is $\varepsilon_{\mathrm{Training}} = 8\%$. Taking these overheads into account, the raw data rate is $R_{\mathrm{Raw}} = 21.6$ Gb/s. With an additional 7% for FEC overhead, the data rate after coding is $R_{\mathrm{Net}} = 20.2$ Gb/s.

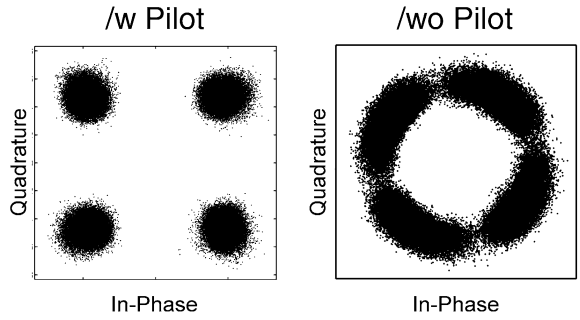

Fig. 2. Vector constellation diagram with and without RF-aided phase noise compensation (overlay of all subcarriers).

III. RF-Aided Phase Noise Compensation Scheme

In a coherent transmission system, a relatively high power local oscillator is mixed with the received signal and the sum is detected by a photodiode thereby downmixing the received optical signal. Coherent detection can either be used to downmix an optical signal directly into its baseband (homodyne detection) or to downmix to an intermediate frequency (heterodyne detection). Although we focus in this work on heterodyne detection, all derived conclusions are valid for homodyne receivers as well.

The phase noise of the lasers used in a coherent optical system has a big impact on the performance. Fig. 2 shows a measured constellation of a 12.9-Gb/s OFDM signal with and without phase noise compensation. In this figure the rotations of the constellation and intercarrier interference (ICI) caused by phase noise can clearly be seen. In several coherent fiber-optic transmission systems carrier phase estimation is performed by using the 4th order nonlinearity [14], [15]. However, for CO-OFDM it has been shown that such a data-aided carrier phase estimation results in a poor performance [3]. Phase noise compensation requirements are more stringent in an OFDM system as the symbol rate (at the same data rate) is significantly lower than that of conventional fiber-optic systems. It has been shown that by using scattered OFDM subcarrier pilots a better phase noise compensation can be realized [3]. Still the linewidth of the lasers used in this experiment was only limited, i.e., 20 kHz, and furthermore a small FFT size of 128 was used.

We recently proposed RF-pilot aided phase noise compensation for OFDM systems [4]. With this technique phase noise compensation is realized by placing an RF-pilot tone in the middle of the OFDM band at the transmitter that is subsequently used at the receiver to revert phase noise impairments. The basic idea behind this phase noise compensation scheme is as follows. When an RF-pilot is inserted at the transmitter, this pilot is distorted by phase noise in exactly the same way as the OFDM signal. Therefore the pilot can be used at the receiver to revert any phase distortions from the OFDM signal. Similar techniques have been reported where an RF-pilot or carrier has been used for laser stabilization [16] or carrier recovery [17], [18]. The main benefit of RF-pilot aided phase noise compensation is that the pilot is placed in the middle of the OFDM signal. Therefore, no extra optical bandwidth needs to be allocated for the

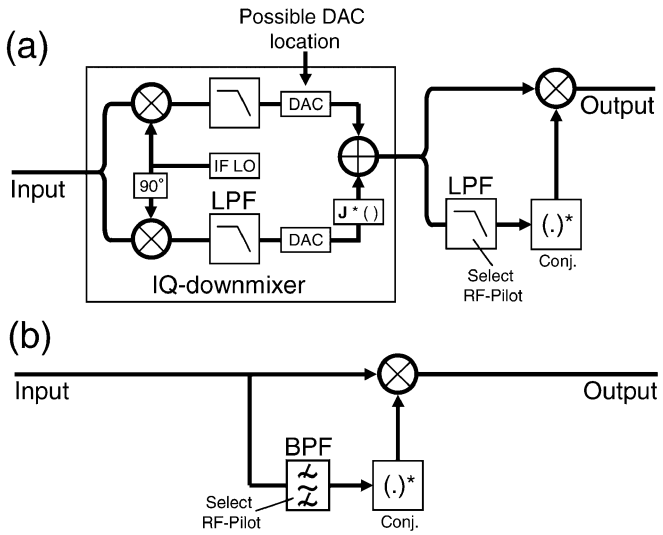

Fig. 3. Two possible implementation for downconversion from the IF into the baseband and phase noise compensation.

RF-pilot. Furthermore, no extra hardware is required at the receiver as the RF-pilot is detected with the same hardware that is used for the OFDM signal as well.

A straightforward method to insert an RF-pilot in the middle of the OFDM signal is by setting the first OFDM channel to 0 and inserting a small dc offset (typically 5 mV) in the I and Q tributaries of the IQ-mixer (In the experimental setup shown in Fig. 5, these offset voltages are $\mathrm{V_{bias\ A}}$ and $\mathrm{V_{bias\ B}}$). The DC offset will be upconverted with the OFDM signal and as a result a small RF-pilot will be present at the IF frequency. In the electrical spectrum after upconversion [Fig. 6(d)] the RF-pilot can clearly be seen.

Fig. 3 shows two possible receiver implementations for IQ downmixing and phase noise compensation. The implementation used in [4] is shown in Fig. 3(a). In this configuration, the OFDM signal is first downconverted into the baseband using a software-based IQ mixer. Subsequently, the phase noise is compensated for by separating the RF-pilot from the OFDM signal with a LPF, applying a complex conjugation to the RF-pilot and multiplying this with the OFDM signal. The main advantage of this approach is that by using an analog RF IQ-mixer, the DAC can be placed after downconversion. This significantly reduces the bandwidth requirements of the DAC as the signal is digitalized after downconversion. In Fig. 3(a), the DAC location of the configuration with the IQ mixer in front of the DAC is marked with "Possible DAC location." Note, however, that in the experiments reported in this paper the DAC was placed before the IQ-downmixer (as shown in Fig. 9) and thus a software based IQ downmixer was implemented.

Fig. 3(b) shows the phase compensation scheme used in [6] and [19]. Here the downconversion and phase noise compensation are combined and thus the RF-pilot tone is used to downmix from the IF into the baseband and for phase noise compensation at the same time. After the DAC, the RF-Pilot is separated from the OFDM signal with a BPF and similar to the configuration shown in Fig. 3(a), the RF-pilot is conjugated and multiplied with the OFDM signal. Note that the performance of both implementations is the same as long as all operations are performed in the digital domain.

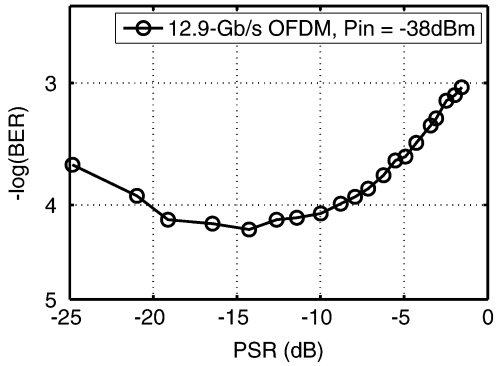

Fig. 4. BER as a function of the pilot-to-signal ratio (PSR).

Both the bandwidth of the electrical filter used to select the RF-pilot tone and the pilot-to-signal ratio (PSR) have a major influence on the receiver performance of the RF-aided pilot compensation scheme. The PSR is defined as

$$\mathrm{PSR[dB]} = 10\log_{10}\left(\frac{P_{\mathrm{RF}}}{P_{\mathrm{OFDM}}}\right). \tag{7}$$

where P_{RF} and P_{OFDM} represent the electrical power of the RF-pilot and the OFDM baseband, respectively. Both the optimum bandwidth of the BPF and the PSR are dependent on the linewidth of the laser [6]. For the ECL lasers used in this experiment with a typical linewidth of 100 kHz, a BPF with 10 MHz bandwidth is optimal [19]. Fig. 4 shows the BER as a function of PSR for a 12.9 Gb/s OFDM system in back-to-back configuration. The received power in this measurement is kept constant at -38 dBm ($\mathrm{OSNR} = 11.2$ dB/0.1 nm) and the PSR is varied from -25 to -2 dB. The best BER is obtained for a PSR of about -15 dB.

For low PSR, the RF-pilot is too weak and amplified spontaneous emission (ASE) noise reduces the degree with which the phase noise can be compensated for, whereas for higher PSR the optical signal-to-noise ratio (OSNR) of the OFDM signal becomes too low. In the transmission experiment described in Section IV, the optimal PSR value of -15 dB is used.

IV. Experimental Setup

A. OFDM Transmitter

The setup used for the OFDM transmission experiment is shown in Fig. 5. The 25.8-Gb/s OFDM signal consists of two subcarrier multiplexed (SCM) OFDM bands that carry 12.9-Gb/s each. Each OFDM baseband signal is generated by a Tektronix AWG7102 AWG. The waveforms produced by the AWG have offline been calculated and are outputted continuously. A digital data stream (PRBS of length $2^{15}-1$) is parallelized and mapped into complex constellation points. In this configuration 4-QAM (QPSK) is used. Subsequently, the OFDM signal is created by taking the IFFT of the mapped symbols. A 27 samples (2.7 ns) cyclic prefix per OFDM symbol is used to increase the tolerance towards synchronization offsets and ISI due to chromatic dispersion.

The sampling rate of the AWG is 10 Gsamples/s, resulting in a bandwidth of 5 GHz. As DACs are used to generate the OFDM baseband, oversampling is required in order to spectrally separate the baseband from high frequency aliasing products. In an OFDM system, oversampling can either be implemented by upsampling the OFDM signal before the DACs or by placing zeros on a number of subcarriers, i.e., at the input to the IFFT. These carriers are sometimes referred to as "zero-subcarriers" or "virtual subcarriers." For practical reasons, the latter technique is implemented. An FFT size of 256 is used. Taking the cyclic prefix into account, this results in a subcarrier data rate of 35.3 MSym/s. Of the 256 channels, 165 are used for data transmission. Channel 1 of the FFT array is set to zero in order to enable RF-pilot phase noise compensation (as explained in Section III) and the last 90 channels of the baseband signal are set to zero for oversampling. In the complex IFFT, the first half of the array corresponds to the positive frequencies whereas the second half corresponds to the negative ones. As illustrated in Fig. 5, the virtual subcarriers are located in the middle of the array as these channels correspond to the high frequency subcarriers after the IFFT operation.

Per AWG, two outputs are used, namely one for the real or in-phase (I) and one for the imaginary or quadrature (Q) part of the waveform. Both I and Q signals have a bandwidth of 3.2 GHz. Fig. 6(a) shows the electrical spectrum of the I channel as it is produced by the AWG. Up to 3.2 GHz the OFDM baseband signal can be seen and for 6.8 GHz and higher aliasing products are present. After the DACs the aliasing products are removed by low-pass filters (LPF) with 3.5-GHz bandwidth. Subsequently, an IQ-mixer upconverts the OFDM signal from the baseband to an intermediate frequency (IF).

Fig. 6(b) shows the electrical spectrum after LPF filtering. Because of the LPF and the frequency characteristic of the AWG, an intensity difference of about 10 dB is present between the first and last subcarrier of the OFDM signal. In a system limited by amplified spontaneous emission (ASE) noise, this intensity difference will result in a different subcarrier-to-noise ratio across the spectrum. Therefore, a preemphasis is used to equalize the transmit power of the OFDM subcarriers. The OFDM baseband signal and the signal after IQ mixing with preemphasis are shown in Fig. 6(c) and (d), respectively. In this paper, the preemphasis is chosen such that the intensity after the IQ mixer is equal for all subcarriers [shown in Fig. 6(d)]. Note that after the IQ mixer, the bandwidth of the signal increases from 3.2 to 6.4 GHz.

The two upconverted 12.9-Gb/s OFDM signals are combined by using a passive 6-dB power combiner. Fig. 7(a) shows the measured electrical spectrum of the two SCM multiplexed OFDM signals. The intermediate frequencies of the SCM channels are 11.5 and 18.7 GHz. The total bandwidth of the 25.8-Gb/s OFDM signal is 13.6 GHz. After combination of the two subcarriers, the signal is amplified and fed to the optical modulator. The electrical driver amplifier is operated just below saturation where it provides an output power of 17.8 dBm. A conventional Mach-Zehnder modulator (MZM) is used for modulation with a bandwidth of 32.6 GHz and $\mathrm{Vpp} = 4.5$ V. The modulator was biased in its transmission null where the optical carrier is completely suppressed. Furthermore, this bias configuration ensures that the modulator is driven in its linear field region where the optical field is proportional to the electrical input voltage [1], [20], [21].

An external cavity laser (ECL) with a typical linewidth of 100 kHz is used as the laser source. Fig. 8(a) shows the optical spectrum after modulation at a 0.01 nm resolution bandwidth. In this spectrum, the residual power of the suppressed carrier can be seen at 1546.85 nm. Left and right of the suppressed carrier, the modulated OFDM band and its image band are present, respectively. The image band is generated because a conventional single-ended MZM is used for modulation [1]. In an OFDM transmission system, the image band reduces the spectral efficiency and the power efficiency. Therefore, an optical bandpass filter (BPF) is used after modulation to suppress the upper sideband of the signal. The optical spectrum after the BPF is shown in Fig. 8(b).

B. Transmission Line

For the transmission experiment a 320-km recirculating loop was employed consisting of four 80-km standard single mode fiber (SSMF) spans with an average span loss of 16 dB. The average dispersion is 18.6 ps/nm/km and the PMD coefficient of the fiber is 0.07 ps/$\sqrt{}$ km. The transmission line is realized without optical dispersion compensation and after every span of SSMF, amplification is provided by a hybrid backward pumped Raman/erbium-doped fiber amplifier (EDFA) structure with an average on/off Raman gain of ~ 6 dB.

C. OFDM Receiver

The heterodyne receiver configuration is shown in Fig. 9. Heterodyne detection is realized with a local oscillator (LO), a 3-dB coupler and a balanced detector (3-dB bandwidth >37 GHz). The typical linewidth of the ECL laser, used as LO, is 100 kHz. As the polarization of the OFDM signal is manually aligned with that of the LO at the receiver, no polarization scrambler is used in the recirculating loop. Without this polarization scrambler the PMD can be artificially increased or decreased. However, in this experiment modern fibers with low PMD (0.07 ps/$\sqrt{}$ km) are used. Furthermore, from (2) it can be concluded that the guard time required to eliminate all ISI caused by PMD equals the maximum DGD. For 4160-km transmission over fibers with a PMD coefficient of 0.07 ps/$\sqrt{}$ km this equals $3.5 * 0.07 * \sqrt{4\,160} = 15.8$ ps. This maximum DGD value is negligible compared to the guard time of 2.7 ns allocated in this OFDM transmission. Therefore, it is realistic to assume that the influence of PMD is negligible over the transmission distances measured. Note that without a loop polarization scrambler, the influence of PDL might be reduced as well. The influence of PDL on OFDM transmission systems is not considered in this experiment and remains a topic for future research.

After heterodyne detection, the signal is sampled with a real-time oscilloscope (Tektronix DPO72004) and processed off-line. The sampling frequency is 50 Gsamples/s and the bandwidth of the oscilloscope is 16 GHz with an effective vertical resolution of approximately 4.5 bits. As the bandwidth of the receiver is lower than the IFs used at the transmitter (TX), the LO is placed 51 pm higher than the wavelength of the TX laser. As

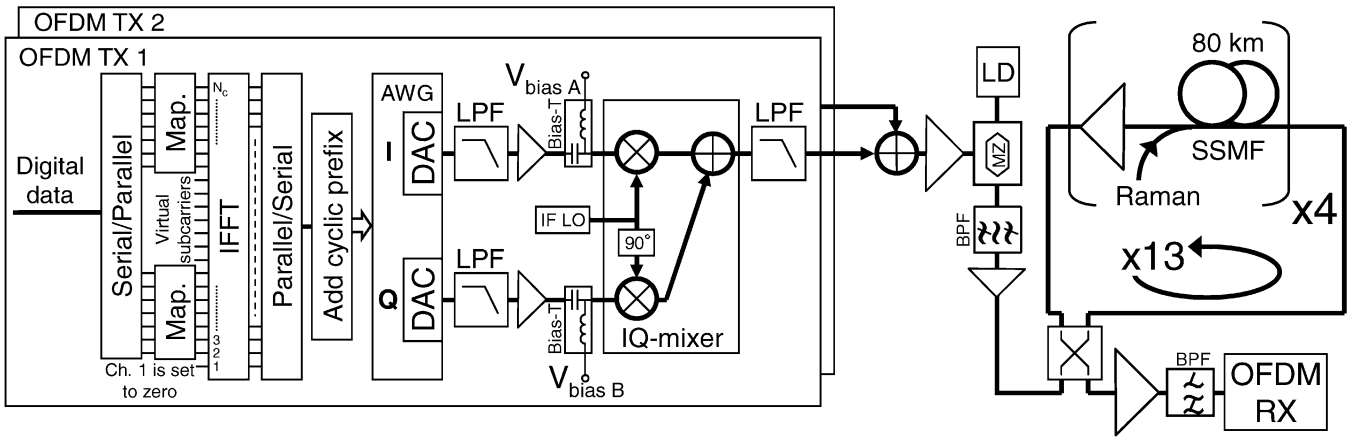

Fig. 5. Transmitter and transmission line of the experimental setup.

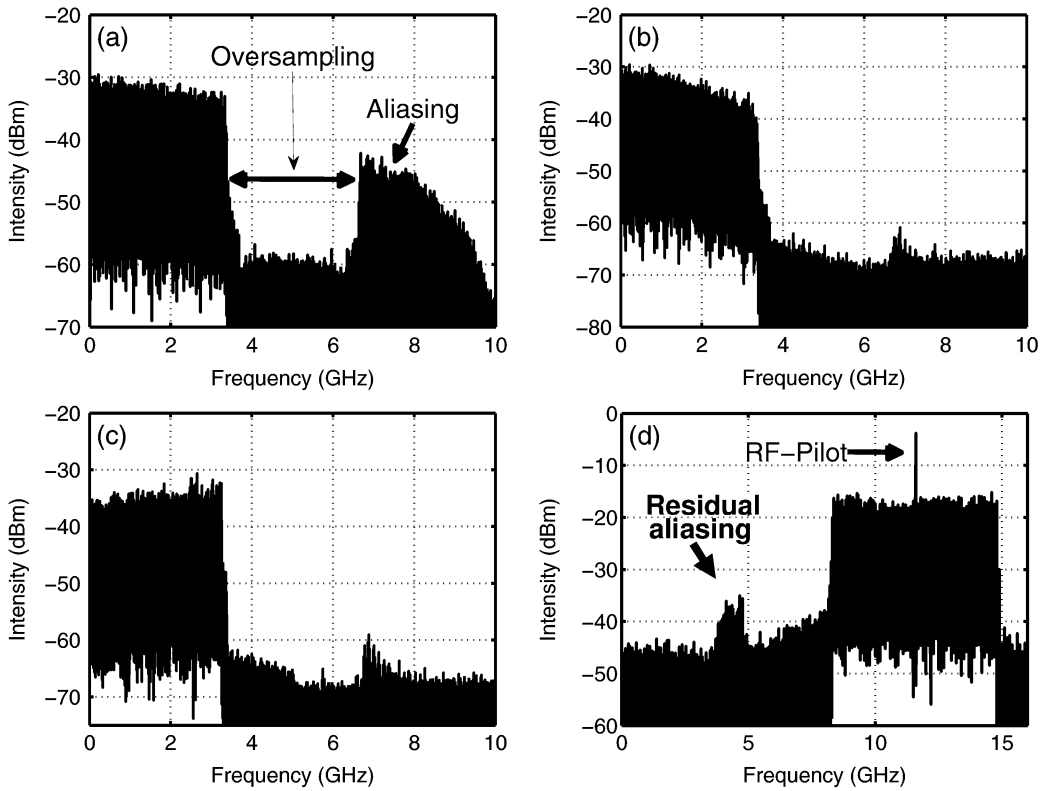

Fig. 6. Electrical spectra at a 10-MHz resolution bandwidth. (a) AWG output. (b) AWG output after LPF. (c) AWG output after LPF with preemphasis. (d) IQ-mixer output with preemphasis.

a result, the IFs of the SCM channels are reduced with 6.4 GHz. The optical spectrum of the OFDM signal combined with the LO is shown in Fig. 8(c). Note that one OFDM SCM band is not visible on the spectrum shown in Fig. 8(c) because of the limited spectral resolution bandwidth of the OSA (0.01 nm). The measured electrical spectrum after balanced detection is shown in Fig. 7(b). Comparing the transmitted [Fig. 7(a)] and received [Fig. 7(b)] electrical spectra, the 6.4 GHz difference in IFs is evident. The optical power of the LO and OFDM signal are 8 and -10 dBm, respectively. After detection with the oscilloscope, the SCM channels are first separated by a BPF. Subsequently they are downconverted and the phase noise of the laser is compensated for using the scheme shown in Fig. 3(a).

As described in Section II, symbol synchronization is realized by dedicated training symbols. After synchronization, the sampling frequency offset is corrected for and the cyclic prefix is removed from the recovered OFDM symbols. Subsequently, the OFDM symbols are converted from serial to parallel and the FFT is applied to convert the signal back into the frequency domain. A one-tap equalizer (1 tap EQ) per subcarrier is used as channel equalizer. As described in Section II this equalizer compensates for timing offsets and chromatic dispersion. Finally, the symbols are demodulated and the bit error-ratio (BER) is computed. For the BERs reported in this paper, more than four million bits per measurement point have been evaluated.

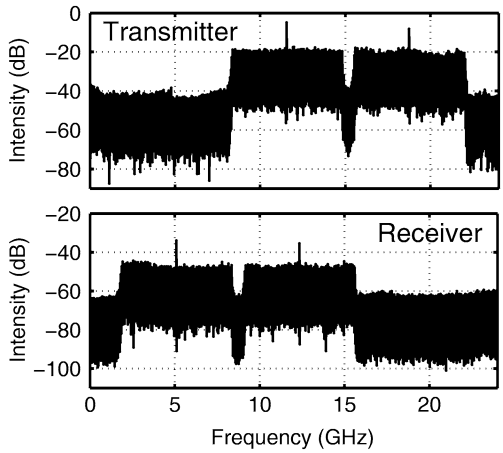

Fig. 7. Electrical spectra at a 10-MHz resolution bandwidth. (a) At the transmitter after multiplexing the two 12.9-Gb/s OFDM bands together. (b) After heterodyne detection with a balanced photodiode.

V. Experimental Results

Fig. 10 shows the back-to-back sensitivity curves for 12.9 and 25.8 Gb/s. A BER of 1×10^{-3} is obtained for an OSNR of 8.9 dB/0.1 nm and 12 dB/0.1 nm for 12.9 Gb/s and 25.8 Gb/s, respectively. Both tributaries of the 25.8-Gb/s sensitivity curve show similar performance and compared to 12.9 Gb/s a 3.1 dB to 4 dB OSNR penalty is observed. The optical spectrum of the 25.8-Gb/s signal is exactly twice as broad and, thus, a 3-dB penalty is expected. In the 25.8-Gb/s configuration additional electrical filters and amplifiers are required, which most likely cause the extra OSNR penalty.

In the transmission experiment training blocks are inserted every 25 OFDM symbols. However, afterwards it has been verified that the symbol spacing can be increased to 200 OFDM symbols without a noticeable difference in BER performance. The BER performance of the 12.9 Gb/s OFDM system with the training-symbol spacing increased to 200 is shown in gray in Fig. 10. Note that in the back-to-back measurement with 200 symbol training-symbol spacing ~ 2 million bits per BER point are evaluated instead of >4 million. With 200 symbol training-symbol spacing the BER performance is slightly better ($\sim$ 0.3-dB OSNR) than the performance when 25 symbol spacing is used. This small improvement is most probably caused by a slightly better adjustment of the transmitter. Increasing the training-symbol spacing from 25 to 200 reduces the overhead from $\varepsilon_{\text{Training}} = 8\%$ to $\varepsilon_{\text{Training}} = 1\%$. As a result, the net data rate of the 12.9-Gb/s OFDM system with 200 symbols training-symbol spacing was 10.8 Gb/s instead of 10 Gb/s.

It is known that transmission systems without inline dispersion compensation exhibit a low nonlinear tolerance because the peak-to-average power ratio (PAPR) is on average higher along the line [22], [23]. For an OFDM signal with 256 subcarriers, the PAPR is inherently higher by about 6–10 dB in comparison to conventional modulation formats. Therefore a low nonlinear tolerance is to be expected for OFDM. Fig. 11 shows the BER as a function of the fiber launch power after 2560-km transmission. The optimum launch power after 2560-km is obtained at a fiber launch power of -4 dBm. Even though this optimum launch power is significantly lower than that for periodically compensated transmission systems (see, for instance, [24]), it is still higher than the optimum launch power for OFDM predicted in simulations [25]. A possible explanation for this difference might be that in our experiment, the noise factor of the EDFAs increased for low fiber launch powers. The EDFAs used for the transmission experiment are designed for output powers of 0 dBm and higher. Fig. 12 shows the measured OSNR after 2560-km transmission and the effective noise factor of the EDFA/Raman amplifiers, derived from the measured OSNR. In optimal operating conditions, the effective noise figure of these amplifiers in combination with 6 dB Raman amplification is about 5 dB. As the optimum launch power is well below the optimal operating condition of the amplifiers, the noise figure of the amplifiers increases for launch powers lower than -3 dBm. The delivered OSNR after 2560-km transmission therefore strongly decreases for low input powers resulting in an offset in the optimum fiber launch power.

Fig. 13 shows the BER as a function of transmission distance (with -4-dBm launch power). After 4160-km transmission a BER of 1.4×10^{-3} is observed, which is just below the expected FEC limit of a concatenated Read-Solomon code with 7% redundancy. After 4000-km transmission, a small acceleration in BER degradation is observed. According to (2), a cyclic prefix of 6.2 ns would be required, in order to compensate for all ISI caused by chromatic dispersion. As the cyclic prefix used in this transmission experiment (2.7 ns) is significantly smaller than this required cyclic prefix, we conjecture that the small acceleration in BER degradation is caused by residual ISI from chromatic dispersion.

VI. Outlook

Long-haul optical transmission links are evolving more and more towards dynamically reconfigurable networks. In such networks it becomes more and more important to use modulation techniques that do not require a complex link design or optimized dispersion map. For such systems OFDM is an effective technique to eliminate virtually all ISI caused by chromatic dispersion and PMD and therefore an ideal candidate to further increase the flexibility of these networks. However, all OFDM transmission experiments reported so far [1]–[4], [19] have been realized with offline generation and detection of the OFDM baseband. In order to realize real time generation and detection of OFDM for high-speed optical transmission, several technical challenges still remain.

The main challenge in OFDM is probably the DACs and ADCs that are required at the transmitter and receiver, respectively. For the 25.8-Gb/s implementation discussed in this paper, DACs with a 3.2-GHz electrical bandwidth and 10-Gsamples/s sampling are used at the transmitter. At the receiver a 15-GHz bandwidth is required to capture both SCM multiplexed OFDM bands in the absence of an analog IQ mixer for downconversion. This requires a minimum ADC sampling rate of about 30-Gsamples/s. With an analog IQ mixer as downconverter, the ADC bandwidth requirements are reduced to 3.2-GHz with a >6.4-Gsamples/s sampling rate. However, the

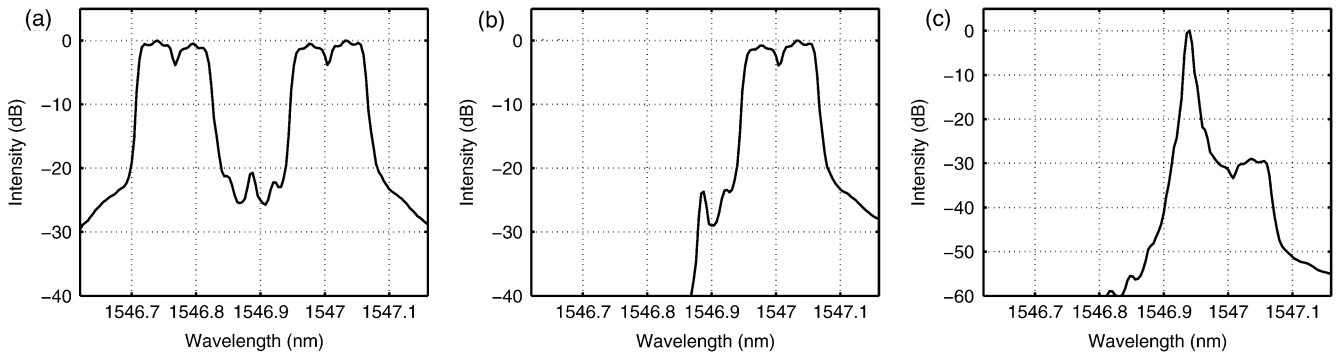

Fig. 8. Optical spectra at 2.5-GHz resolutions bandwith. (a) After modulation. (b) After SSB filtering. (c) At the receiver just before the balanced photodiode.

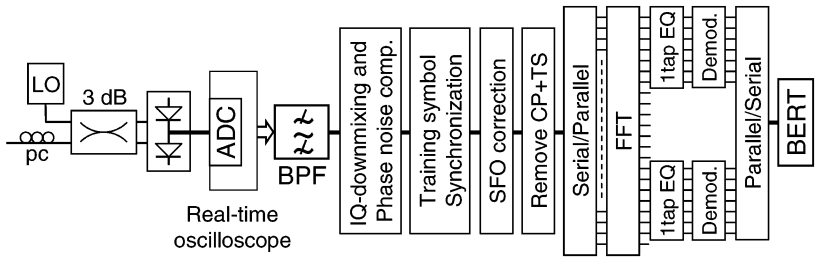

Fig. 9. Experimental setup of the heterodyne detector and software implementation of the OFDM receiver.

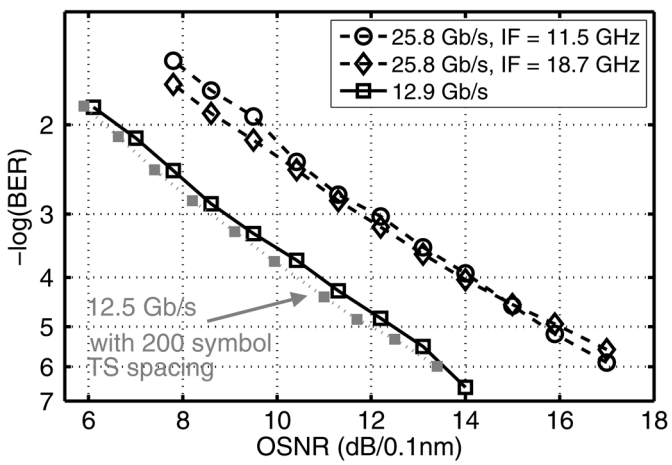

Fig. 10. BER as a function of the OSNR in back-to-back configuration.

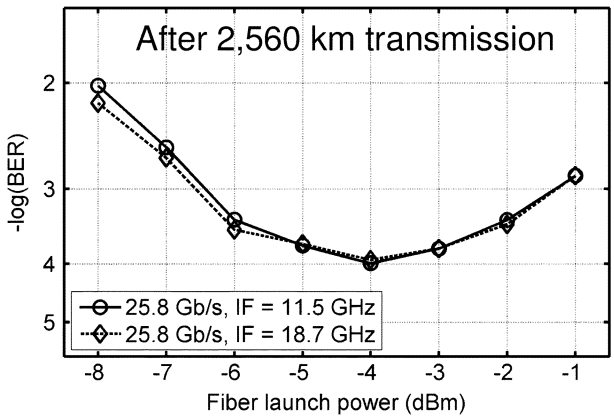

Fig. 11. BER as a function of the fiber launch power measured after 2560-km transmission.

receiver complexity increases significantly as more analog components are added to the RF receiver front-end. Furthermore, to use analog down-mixing for the 25.8-Gb/s implementation discussed in this paper, two ADCs per subband (a total of 4 ADCs) would have been required to detect the in-phase and quadrature component of the IQ-mixer independently, instead of a single ADC without analog downmixing.

A further concern is the vertical resolution of the ADC and DACs. The question remains what the minimum vertical resolution is required to generate and detected an OFDM signal. All experiments reported so far have used high precision AWGs and oscilloscopes for the generation and detection of the OFDM signal. Additionally, the precision of offline processing is significantly higher than what normally would be realized within a dedicated hardware implementation.

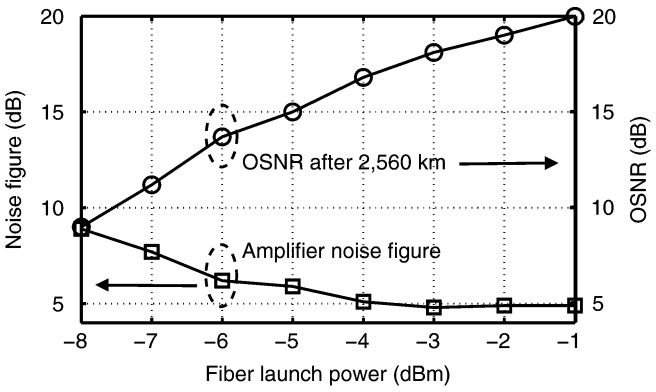

Fig. 12. Noise figure of the EDFA/Raman combination and the OSNR after 2560-km transmission as a function of the fiber launch power.

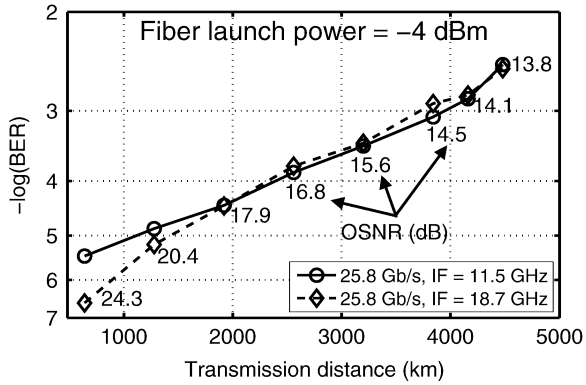

Fig. 13. BER as a function of the transmission distance for a fiber launch power of -4 dBm.

Besides OFDM, other technologies that rely heavily on digital signal processing have gained significant interest in optical transmission. The best example is coherent equalization [15], [26]–[28], which combines digital equalization with coherent detection. When this is combined with multilevel modulation formats and polarization multiplexing (POLMUX), the symbol rate can be reduced enough to realize 40-Gb/s [15], [26], [27] and even 100-Gb/s [28] optical transmission together with digital equalization techniques. OFDM and coherent equalization with DQPSK modulation are similar to the extent that they in principle allow complete compensation of ISI in the electrical domain. Compared to digital equalization, the main advantage of OFDM is that the number of numerical operations required in the DSP can be reduced and that therefore a more cost-effective implementation of OFDM might be possible [29]. The main drawback of OFDM is the inherently higher PAPR, which reduces the nonlinear tolerance in comparison to DQPSK. Further research in both OFDM and DQPSK transmission is still required to understand the principle limitations in nonlinear tolerance.

To summarize, OFDM has shown to greatly increase the flexibility and data throughput in wireless communication networks. We therefore speculate that long-haul fiber-optic transmission is the next application that will benefit from OFDM to increase transmission performance and flexibility.

VII. Conclusion

In this paper, long-haul transmission of a coherent optical OFDM transmission system is discussed. A novel method to compensate for laser phase noise in coherent systems is introduced. With this compensation scheme 25.8-Gb/s CO-OFDM transmission is realized over 4160 km without dispersion compensation. Along the whole link, the OFDM signal is continuously detectable demonstrating a dispersion tolerance of more than 77 000 ps/nm. Such a large dispersion tolerance is attractive for high speed transmission systems as it eliminates the necessity of inline dispersion compensation even in dynamically reconfigurable networks.

Acknowledgment

The authors would like to thank D. van den Borne from the Eindhoven University of Technology, The Netherlands, for the many fruitful discussions. Furthermore, the authors thank Dr. S. Akiba, Dr. M. Suzuki, and Dr. M. Usami from KDDI R&D Laboratories for their support.

References

[1] B. J. C. Schmidt, A. J. Lowery, and J. Armstrong, "Experimental demonstrations of 20 Gbit/s direct-detection optical OFDM and 12 Gbit/s with a colorless transmitter," in *Proc. Opt. Fiber Commun. Conf.*, Anaheim, CA, 2007, Paper PDP 18.

[2] S. C. J. Lee, F. Breyer, S. Randel, M. Schuster, J. Zeng, F. Huijskens, H. P. A. van den Boom, A. M. J. Koonen, and N. Hanik, "24-Gb/s transmission over 730 m of multimode fiber by direct modulation of an 850-nm VCSEL using discrete multi-tone modulation," in *Proc. Opt. Fiber Commun. Conf.*, Anaheim, CA, 2007, Paper PDP 6.

[3] W. Shieh, X. Yi, and Y. Tang, "Transmission experiment of multi-gigabit coherent optical OFDM systems over 1000 km SSMF fibre," *Electron. Lett.*, vol. 43, no. 3, pp. 183–184, 2007.

[4] S. L. Jansen, I. Morita, N. Takeda, and H. Tanaka, "20-Gb/s OFDM transmission over 4160-km SSMF enabled by RF-pilot tone phase noise compensation," in *Proc. Opt. Fiber Commun. Conf.*, Anaheim, CA, 2007, Paper PDP 15.

[5] T. C. W. Schenk, R. W. van der Hofstad, E. R. Fledderus, and P. F. M. Smulders, "Distribution of the ICI term in phase noise impaired OFDM systems," *IEEE Trans. Wireless Commun.*, vol. 6, no. 4, pp. 1488–1500, Apr. 2007.

[6] S. L. Jansen, I. Morita, and H. Tanaka, "10-Gb/s OFDM with conventional DFB lasers," in *Proc. Europ. Conf. Opt. Commun.*, Berlin, Germany, 2007, Paper Tu. 2.5.2.

[7] J. G. Proakis, *Digital Communications*, 4th ed. New York: McGraw-Hill, 2001.

[8] A. J. Lowery and J. Armstrong, "Orthogonal-frequency-division multiplexing for optical dispersion compensation," in *Proc. Opt. Fiber Commun. Conf.*, Anaheim, CA, 2007, Paper OTuA4.

[9] R. van Nee and R. Presad, *OFDM for Wireless Multimedia Communications*. Norwood, MA: Artech House, 2000.

[10] T. C. W. Schenk, M. M. de Laat, P. F. M. Smulders, and E. R. Fledderus, "Symbol timing for multiple antenna OFDM systems," in *Proc. IEEE Veh. Technol. Conf.*, 2006, vol. 3, pp. 1521–1525.

[11] T. M. Schmidl and D. C. Cox, "Robust frequency and timing synchronization for OFDM," *IEEE Trans. Commun.*, vol. 45, no. 12, pp. 1613–1621, 1997.

[12] M. Sliskovic, "Carrier and sampling frequency offset estimation and correction inmulticarrier systems," in *Proc. GLOBECOM 2001*, vol. 1, pp. 285–289.

[13] W. Shieh and C. Athaudage, "Coherent optical orthogonal frequency division multiplexing," *Electron. Lett.*, vol. 42, no. 10, pp. 587–589.

[14] S. Tsukamoto, D.-S. Ly-Gagnon, K. Katoh, and K. Kikuchi, "Coherent demodulation of 40-Gbit/s polarization-multiplexed QPSK signals with 16-GHz spacing after 200-km transmission," in *Proc. Opt. Fiber Commun. Conf.*, Anaheim, CA, 2007, Paper PDP 29.

[15] S. J. Savory, G. Gavioli, R. I. Killey, and P. Bayvel, "Electronic compensation of chromatic dispersion using a digital coherent receiver," *Opt. Express*, vol. 15, no. 5, pp. 2120–2126.

[16] O. Solgaard, J. Park, J. B. Georges, P. K. Pepeljugoski, and K. Y. Lau, "Millimeter wave, multigigahertz optical modulation by feedforward phase noise compensation of a beat note generated by photomixing of two laser diodes," *IEEE Photon. Technol. Lett.*, vol. 5, no. 5, pp. 574–577, 1993.

[17] W. Shieh and W. Chen, "Optical carrier recovery using feedforward phase compensation," in *Europ. Conf. Opt. Commun.*, vol. 3, pp. 654–655.

[18] M. Nakazawa, J. Hongo, K. Kasai, and M. Yoshida, "Polarization-multiplexed 1 gsymbol/s, 64 QAM (12 Gbit/s) coherent optical transmission over 150 km with an optical bandwith of 2 GHz," in *Proc. Optical Fiber Commun. Conf.*, Anaheim, CA, 2007, Paper PDP 26.

[19] S. L. Jansen, I. Morita, N. Takeda, and H. Tanaka, "Pre-emphasis and RF-pilot tone phase noise compensation for coherent OFDM transmission systems," in *Proc. IEEE/LEOS Summer Top. Meet.*, 2007, Invited, MA1.2.

[20] M. L. Farwell, W. S. C. Chang, and D. R. Huber, "Increased linear dynamic range by low biasing the Mach-Zehnder modulator," *IEEE Photon. Technol. Lett.*, vol. 5, no. 7, pp. 779–782, 1993.

[21] Y. Tang, W. Shieh, X. Yi, and R. Evans, "Optimum design for RF-to-optical up-converter in coherent optical OFDM systems," *IEEE Photon. Technol. Lett.*, vol. 19, no. 7, pp. 483–485, 2007.

[22] R. J. Essiambre and P. J. Winzer, "Impact of fiber nonlinearities on advanced modulation formats using electronic pre-distortion," in *Proc. Opt. Fiber Commun. Conf.*, Anaheim, CA, 2006, Paper OWB1.
[23] A. Klekamp, F. Buchali, M. Audoin, and H. Bülow, "Nonlinear limitations of electronic dispersion pre-compensation by intrachannel effects," presented at the Opt. Fiber Commun. Conf., Anaheim, CA, 2006, Paper OWR1.
[24] M. Suzuki and N. Edagawa, "Dispersion-managed high-capacity ultra-long-haul transmission," *J. Lightw. Technol.*, vol. 21, no. 4, pp. 916–929, 2003.
[25] A. J. Lowery, L. B. Du, and J. Armstrong, "Performance of optical OFDM in ultralong-haul WDM lightwave systems," *J. Lightw. Technol.*, vol. 25, no. 1, pp. 131–138, 2007.
[26] C. Laperle, B. Villeneuve, Z. Zhang, D. McGhan, H. Sun, and M. O'Sullivan, "Wavelength division multiplexing (WDM) and polarization mode dispersion (PMD) performance of a coherent 40 Gbit/s dual-polarization quadrature phase shift keying (DP-QPSK) transceiver," in *Proc. Opt. Fiber Commun. Conf.*, Anaheim, CA, 2007, Paper PDP 16.
[27] G. Charlet, J. Renaudier, M. Salsi, H. Mardoyan, P. Tran, and S. Bigo, "Efficient mitigation of fiber impairments in an ultra-long haul transmission of 40 Gbit/s polarization-multiplexed data by digital processing in a coherent receiver," in *Proc. Opt. Fiber Commun. Conf.*, Anaheim, CA, 2007, Paper PDP 17.
[28] C. R. S. Fludger, T. Duthel, D. van den Borne, C. Schulien, E.-D. Schmidt, T. Wuth, E. de Man, G. D. Khoe, and H. de Waardt, "10 $\times$ 111 Gbit/s, 50 GHz spaced, POLMUX-RZ-DQPSK transmission over 2375 km employing coherent equalization," in *Proc. Opt. Fiber Commun. Conf.*, Anaheim, CA, 2007, Paper PDP 22.
[29] H. Bulow, "Tutorial electronic dispersion compensation," in *Proc. Opt. Fiber Commun. Conf.*, Anaheim, CA, 2007, Paper OMG5.

Sander L. Jansen (S'02–M'07) was born in Maartensdijk, The Netherlands, in 1978. He received the M.Sc. and Ph.D. degrees (*cum laude*) in electric engineering from the University of Technology, Eindhoven, The Netherlands. Both the Master's degree thesis and Ph.D. degree research were conducted at Siemens AG, Munich, Germany. His Master's degree thesis was part of the European-funded Information Society Technologies (IST) project FASHION where he worked on ultrafast optical signal processing. The main research focus of his Ph.D. degree was phase conjugation for long-haul transmission systems.

Since September 2006, he has been working as an Associate Research Engineer with KDDI R&D Laboratories, Saitama, Japan, where he specialized in OFDM for fiber-optic transmission systems. His main research interests are modulation formats, OFDM, coherent detection, and fiber-optic transmission systems. He authored and coauthored more than 60 refereed papers and conference contributions.

Dr. Jansen was awarded the IEEE Lasers and Electro-Optics Society (LEOS) Graduate Student Fellowship in 2005.

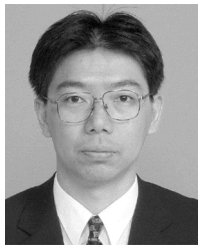

Itsuro Morita received the B.E., M.E., and Dr. Eng. degrees in electronics engineering from the Tokyo Institute of Technology, Tokyo, Japan, in 1990, 1992, and 2005, respectively.

He joined Kokusai Denshin Denwa (KDD) Company Ltd. (currently KDDI Corporation), Tokyo, in 1992 and, since 1994, he has been with their Research and Development Laboratories. He has been engaged in research on long-distance and high-speed optical communication systems. In 1998, he was on leave at Stanford University, Stanford, CA.

Tim C. W. Schenk (S'01–M'07) received the M.Sc. and Ph.D. degrees in electrical engineering from Eindhoven University of Technology (TU/e), Eindhoven, The Netherlands, in 2002 and 2006, respectively. The dissertation topic for his Ph.D. degree concerned the digital compensation of front-end impairments in multiple-antenna multicarrier systems.

From 2002 to 2004, he was with the Wireless Systems Research Group of Agere Systems, Nieuwegein, The Netherlands. From 2004 to 2006, he was a Research Assistant with the Radiocommunications Group, TU/e. In October 2006, he joined the Connectivity Systems and Networks Department, Philips Research Laboratories, Eindhoven, as a Research Scientist. His current interests include wireless communications and signal processing.

Dr. Schenk was awarded the 2006 Veder Award from the Dutch Scientific Radio Fund Veder for the work related to his Ph.D. degree thesis. He is a member of the Royal Institute of Engineers (KIvI) in The Netherlands and the Dutch Electronics and Radio Society (NERG).

Noriyuki Takeda received the B.S. and M.S. degrees in communication engineering from Osaka University, Osaka, Japan, in 1991 and 1993, respectively.

In 1993, he joined Kokusai Denshin Denwa (KDD) Ltd. (currently the KDDI Corporation), Tokyo. Since August 2006, he has been with the Optical Network Architecture Group. His main research activities are advanced modulation formats and fiber-optic transmission systems, as well as the standardization of 100 GbE.

Hideaki Tanaka was born in Osaka, Japan, on April 5, 1961. He received the B.E., M.E., and Ph.D. degrees in electronics engineering from Osaka University, in 1984, 1986, and 1997, respectively.

In 1986, he joined Kokusai Denshin Denwa (KDD) R&D Laboratories (currently KDDI R&D Laboratories), Tokyo, Japan. Since 1986, he has been engaged in research on high-speed semiconductor modulators, their integrated devices and design of optical submarine cable systems, optical access technologies, and generalized multiprotocol label switching (GMPLS) technologies. Currently, he is the Senior Manager with the Optical Network Architecture Laboratory, KDDI R&D Laboratories, Inc., Saitama, Japan.

Dr. Tanaka received the Best Paper award from Opto-Electronics Conference (OEC) in 1988, the Young Engineering Award from Institute of Electronics, Information, and Communication Engineers (IEICE) in 1993, and the distinguished paper award from IEICE in 1995.